Vertical Graphene Tunneling Heterostructure with Ultrathin Ferroelectric $BaTiO_3$ Film as a Tunnel Barrier

*Hung-Lit Chan, Shuoguo Yuan, and Jianhua Hao**

Department of Applied Physics, The Hong Kong Polytechnic University, Hong Kong, P. R. China

*Corresponding author. E-mail: **jh.hao@polyu.edu.hk**

Keywords: two-dimensional materials, pulsed laser deposition, ferroelectric tunnel junctions, tunneling electroresistance effect, graphene-based devices

Abstract: Ferroelectric tunnel junctions (FTJs) have attracted enormous interests as one of the promising candidates for next-generation non-volatile resistance memories. In this work, we report a novel FTJ employing both two-dimensional material and semiconductor electrode, in the graphene/BaTiO3/Nb:SrTiO3 heterostructure, yielding an interesting tunneling electroresistance (TER) effect. We investigate the TER dependence on Nb doping concentrations from 0.1 wt% to 1.0 wt% in the semiconductor electrode. In addition to modulating barrier height by ferroelectric polarization reversal, the ON/OFF resistance ratio can be tuned by adjusting Nb doping concentrations due to further modulation of barrier width. An optimized ON/OFF ratio above 10^3 of the device is observed when introducing 0.1 wt% Nb concentration at room temperature. Furthermore, good retention property and switching reproducibility can be achieved in the devices. The results provide a novel pathway to design the graphene-based FTJ at the nanoscale, which is useful for developing non-volatile memory devices with enhanced performance.

Introduction

Ferroelectric tunnel junctions (FTJs) have received extensive attention for non-volatile memory application with non-destructive resistive readout, high data storage density and simple device architecture.[1-3] FTJs are composed of an ultrathin ferroelectric film sandwiched between two electrodes.[4-7] The polarization reversal in the ferroelectric barrier results in the switching of the resistance between a high (OFF state) and a low (ON state) value. The effect is known as tunneling electroresistace (TER).[8-10] Various FTJs employing metal electrodes have demonstrated the TER effect, such as Pt/$BaTiO_3$(BTO)/$SrRuO_3$,[11] where the ON/OFF conductance ratio is attributed to the ferroelectric modulation of barrier height. According to basic quantum mechanics, the tunneling transmission of electrons passing through the ferroelectric barrier is exponentially dependent on the barrier width, in addition to the barrier height. The TER is expected to be increased when the barrier width can be further modulated.[15, 16] Recently,FTJs using the semiconductor electrode, Nb-doped $SrTiO_3$ (NSTO), have been reported in Pt/BTO/NSTO.[17] A giant TER has been observed due to the barrier width modulation. Therefore, the use of a semiconductor electrode is an efficient approach to tune the transport properties of the junction device.

It is well known that graphene, a zero-bandgap two-dimensional material, exhibits various outstanding properties, such as high carrier mobility, thermal conductivity, mechanical strength and impermeability with gas and liquid.[18-20] Graphene is widely used as single-atom-thick and transparent electrodes for electronic and optoelectronic devices.[21] However,

there has been limited study on the device design using both graphene electrode and semiconductor electrode. Our recent study implies that high performance can be achieved in a graphene-based field-effect transistor based on Au/$BiFeO_3$/graphene on an oxidized Si by

tuning transport properties of the multilayer structure.[22] Therefore, it is expected that employment of semiconducting electrodes may further manipulate the resistance switching of the graphene-based FTJs. In this work, we investigate electrical resistance switching in the novel graphene/BTO/NSTO heterostructure. The ON/OFF conductance ratio is found to increase with decreasing Nb concentration from 1.0 wt% to 0.1 wt% on the semiconductor electrode. A remarkable ON/OFF ratio up to 10^3 is observed in the device when introducing Nb concentration of 0.1 wt% at room temperature. These observations show the ferroelectric-driven barrier tunability in terms of both height and width on the semiconductor interface to enhance TER performance of graphene-based FTJs. Furthermore, good retention property and switching reproducibility can be obtained in the devices, which may facilitate the design of non-volatile memory applications.

Experiments

Pulsed laser deposition (PLD) has proved to be a conventional technique in depositing high-quality titanate thin films.[23, 24] Here, 3 nm-thick BTO thin films were grown on (001)-oriented NSTO single crystal substrates by PLD method. The NSTO substrates with different Nb doping concentration of 0.1 wt%, 0.7 wt% and 1.0 wt% were used. During deposition, a KrF excimer laser was focused on a high-purity BTO target with the wavelength of 248 nm, fluence of 250 mJ and repetition rate of 1 Hz. The BTO films were grown at deposition temperature of 700 °C under oxygen pressure of 10 Pa. After deposition, the thin films were

cooled down to room temperature. The purchased CVD-grown graphene/copper sheets were spin-coated with poly (methyl methacrylate) (PMMA), cut into small pieces and etched with ammonium persulfate for 12 hrs. The PMMA-coated graphene layers were transferred onto BTO/NSTO heterostructure by a standard wet transfer technique. After removing the PMMA with acetone, Au dots with 100 μm diameter were prepared on the samples by thermal evaporation through a shadow mask. The Raman spectroscopy of graphene layers was

obtained by high-resolution Raman system (Horiba, LabRAM HR 800) using a laser excitation source with a wavelength of 488 nm. The X-ray photoelectron spectroscopy (XPS) characterization was performed on the X-ray photoelectron spectrometer (Thermo Scientific, ESCALAB 250Xi). The piezoresponse force microscopy (PFM) measurement of BTO films was conducted using an atomic force microscope (Asylum Research, MFP-3D infinity). The electrical resistance switching of the devices was measured at room temperature using a probe station connected to a Keithley 4200-SCS semiconductor parameter analyzer.

Results and discussion

Figure 1(a) exhibits the topography of the graphene/BTO/NSTO tunnel junction with smooth surface of a root-mean-square roughness of around 0.19 nm. The corresponding device geomety is shown in the inset. **Figure 1**(b) reveals the Raman spectrum of the CVD-grown graphene used for transfer on BTO/NSTO heterostructure. Two active features of G peaks and 2D peaks can be identified. A symmetric 2D peak centers at about 2695 cm^{-1} with a full-width-at-half-maximum (FWHM) of around 30 cm^{-1}. The intensity of the 2D peak is found to be approximately two times higher than that of the G peak, which confirms the graphene is a single layer. An insignificant defect peak observed suggests high quality of the graphene layer. **Figure 1**(c) shows the XPS measurement of the BTO thin film. Two strong peaks of Ti 2p core level can be observed at 458.3 eV and 464.0 eV, implying the presence of Ti^{4+} ionic state. Two peaks of Ba 3d can be seen at 778.5 eV and 793.8 eV. The atomic ratio

of Ba to Ti is around 1:1. The result in line with reported typical XPS data[25, 26] observed in BTO indicates high quality of the BTO thin film grown by PLD. The ferroelectric characterization of the BTO thin film grown on NSTO substrate (Nb: 0.7 wt%) was revealed by PFM. **Figure 1**(d,e) exhibit the out-of-plane PFM amplitude and phase images of BTO film respectively. The ferroelectric domains are written by applying positive and negative DC voltages of 3 V through a conductive tip on the BTO surface. As observed from the phase

image, the purple regions represent the upward domains where the polarization points away from the NSTO substrate after application of a negative poling voltage. The yellow regions mean the downward domains where the polarization points towards the NSTO with an applied positive poling voltage. The 180° phase contrast reveals the antiparallel polarization in the two domains. The local PFM hysteresis loops further confirm the ferroelectric nature with switchable polarization of the BTO thin film, as shown in **Figure 1**(f).

To study the TER effect of graphene/BTO/NSTO heterostructure, two-terminal geometry was employed for current-voltage (*I-V*) characterization at room temperature. The applied voltage is termed as positive direction when a positive bias is applied to the graphene electrode. The NSTO electrode was grounded for all electrical measurement. **Figure 2**(a,b) show the *I-V* curves for the ON state and the OFF state of the graphene/BTO/NSTO heterostructure as a function of Nb concentration in the semiconductor electrode. After applying a positive or negative write voltage pulse V_{write} with pulse width of 0.5 s to the graphene electrode, the *I-V* curve was measured in a low-bias regime (-0.2 V to 0.2 V) at room temperature. The applied voltages are +2.5/-2.5 V, +3.0/-3.0 V and +4.5/-5.0 V for the devices with 1.0 wt%, 0.7 wt% and 0.1 wt% respectively. When a positive voltage is larger than that of ferroelectric coercivity, downward polarization is created in the BTO film. The device is set to low resistance ON state. Similarly, a larger negative voltage drives the device to high resistance OFF state with upward polarization. It is seen from the *I-V* curves that the ON state current is much larger than the OFF state current for all the devices with 1.0 wt%,

0.7 wt% and 0.1 wt%. The clear conductance contrast confirms that the ferroelectric polarization reversal happens. When the Nb concentration changes from 1.0 wt% to 0.1 wt%, the magnitude of the OFF state current decreases sharply from around 10^{-6} to 10^{-8} A, but the ON state current magnitude reduces slightly from 10^{-4} to 10^{-5} A. Consequently, the ON/OFF ratio taken at 0.2 V increases with decreasing Nb concentration, as shown in **Figure 2**(c). A

remarkable ON/OFF ratio about 10^3 can be observed at 0.1 wt% Nb concentration of the novel graphene/BTO/NSTO FTJ, which is about one to two orders higher than that reported in typical BTO-based FTJs with metal electrodes.[11, 12, 27, 28] The schematic resistance switching of graphene/BTO/NSTO heterostructure is revealed in **Figure 2**(d). When a positive voltage pulse drives the polarization pointing towards the NSTO electrode, the depleted region is decreased or even eliminated by electron accumulation on the semiconductor surface. The tunneling barrier height is decreased. The device is switched to the ON state. When a negative voltage pulse is applied, ferroelectric polarization points away from the NSTO electrode. The depleted region on the NSTO surface is enhanced by electron depletion. The depletion region represents an extra tunneling barrier, which increases in both barrier height and width. The device is switched to the OFF state. As wider depletion regions are formed on lower Nb doping semiconductor in the OFF state, which largely increase the barrier height and barrier width, [29] more significant reduction of the OFF state current is expected at the lower Nb concentration, which in turns increases the ON/OFF ratio with decreasing Nb concentration as observed in the graphene/BTO/NSTO devices.

Figure 3 shows the non-volatile resistance-voltage (*R*-*V*) hysteresis loops of graphene/BTO/NSTO heterostructure at room temperature. After applying different write pulses V_{write} with a step of 0.5 V, the resistance was recorded at a fixed read pulse V_{read} of 0.2 V. The obtained *R*-*V* loops exhibit resistive-switching behavior near the coercivity of PFM hysteresis loops in **Figure 1**(f). The observation indicates that the FTJ resistance switching

behaviors are direct results of the ferroelectric polarization switching of the BTO film. It is shown that the positive and the negative write pulses drive the devices to the low resistance state and high resistance state respectively. A positive pulse switches the polarization of BTO to a downward direction, while a negative pulse switches the polarization to an upward direction. When the Nb concentration decreases from 1.0 wt% to 0.1 wt%, it can be seen from the *R-V* loops that the magnitude of the OFF state resistance increases significantly, but the

resistance magnitude of the ON state changes slightly. As a result, the ON/OFF ratio increases with decreasing Nb concentration. For the 0.1 wt% device, a remarkable ON/OFF ratio above 10^3 can be obtained. The ON/OFF ratio enhancement observed in the *R-V* loops is similar to the estimation of the *I-V* curves as described above.

Furthermore, retention property and switching reproducibility are important parameters in non-volatile memory applications. **Figure 4**(a) reveals the resistance retention of graphene/BTO/NSTO heterostructure as a function of Nb concentration. There is no obvious degradation of resistance in both ON state and OFF state within 10^2 s. **Figure 4**(b) exhibits the bipolar resistance switching of the devices with different Nb concentration. The switching characteristics were tested via the repeated bipolar electrical pulses. The write pulse V_{write} height was determined from the *R-V* hysteresis loops for each Nb wt% and read pulse V_{read} of 0.2 V remained unchanged. For the 0.1 wt% device, a high ON/OFF ratio about 10^3 could still be preserved after several write/read cycles. The 0.7 wt% and 1.0 wt% devices with lower ON/OFF ratios also show the good switching endurance.

Conclusions

In summary, a novel FTJ employing both two-dimensional material and semiconductor electrode has been developed in graphene/BTO/NSTO heterostructure. Compared with traditional metal electrodes, graphene electrodes possess the advantages of atomic level thickness and optical transparency, which may facilitate the design of future ultra-broadband and high-speed optoelectronic devices. By modulating Nb doping concentration, the

employment of semiconductor electrodes enables barrier tunability in both height and width responding to polarization reversal to optimize the ON/OFF resistance ratio of the graphene-based FTJs. Moreover, good retention property and switching reproducibility can be observed in the novel graphene/BTO/NSTO heterostructure, which is helpful for developing non-volatile memory at nanoscale.

Acknowledgements

The research was supported by the grant from Research Grants Council of Hong Kong (GRF No. PolyU 153031/15P).

References

1. J. F. Scott, *Science* **2007**, 315, 954.
2. V. Garcia, M. Bibes, *Nature Commun*. **2014**, 5, 4289.
3. R. Guo, L. You, Y. Zhou, Z. S. Lim, X. Zou, L. Chen, R. Ramesh, J. Wang, *Nature Commun*. **2013**, 4, 1990.
4. A. Chanthbouala, A. Crassous, V. Garcia, K. Bouzehouane, S. Fusil, X. Moya, J. Allibe, B. Dlubak, J. Grollier, S. Xavier, C. Deranlot, A. Moshar, R. Proksch, N. D. Mathur, M. Bibles, A. Barthélémy, *Nature Nanotechnol*. **2012**, 7, 101.
5. R. Soni, A. Petraru, P. Meuffels, O. Vavra, M. Ziegler, S. K. Kim, D. S. Jeong, N. A. Pertsev, H. Kohlstedt, *Nature Commun*. **2014**, 5, 5414.
6. R. Guo, Y. Wang, H. Y. Yonng, J. Chai, H. Wang, W. Lin, S. Chen, X. Yan, T. Venkatesan, Ariando, A. Gruverman, Y. Wu, J. Chen, *ACS Appl. Mater. Interfaces* **2017**, 9, 5050.
7. Y. W. Yin, J. D. Burton, Y.-M. Kim, A. Y. Borisevich, S. J. Pennycook, S. M. Yang, T. W. Noh, A. Gruverman, X. G. Li, E. Y. Tsymbal, Q. Li, *Nature Mater*. **2013**, 12, 397.

M. Bibes, *Nature* **2009**, 460, 81.

11. Z. Wen, L. You, J. Wang, A. Li, D. Wu, *Appl. Phys. Lett.* **2013**, 103, 132913.

8. B. B. Tian, J. L. Wang, S. Fusil, Y. Liu, X. L. Zhao, S. Sun, H. Shen, T. Lin, J. L. Sun, C. G. Duan, M. Bibes, A. Barthélémy, B. Dkhil, V. Garcia, X. J. Meng, J. H. Chu, *Nature Commun*. **2016**, 7, 11502.

9. D. Pantel, M. Alexe, *Phys*. *Rev*. *B* **2010**, 82, 134105.

10. V. Garcia, S. Fusil, K. Bouzehouane, S. Enouz-Vedrenne, N. D. Mathur, A. Barthélémy, M. Bibes, *Nature* **2009**, 460, 81.

11. Z. Wen, L. You, J. Wang, A. Li, D. Wu, *Appl. Phys. Lett.* **2013**, 103, 132913.

12. A. Zenkevich, M. Minnekaev, Yu. Matveyev, Yu. Lebedinskill, K. Bulakh, A. Chouprik, A. Baturin, K. Maksimova, S. Thiess, W. Drube, *Appl. Phys. Lett.* **2013**, 102, 062907.

13. D. Pantel, H. Lu, S. Goetze, P. Werner, D. Jik Kim, A. Gruverman, D. Hesse, M. Alexe, *Appl. Phys. Lett.* **2012**, 100, 232902.

14. M. Hambe, A. Petraru, N. A. Pertsev, P. Munroe, V. Nagarajan, H. Kohlstedt, *Adv. Funct. Mater.* **2010**, 20, 2436.

15. M. Y. Zhuravlev, R. F. Sabirianov, S. S. Jaswal, E. Y. Tsymbal, *Phys. Rev. Lett.* **2005**, 94, 246802.

16. X. Liu, J. D. Burton, E. Y. Tsymbal, *Phys. Rev. Lett.* **2016**, 116, 197602.

17. Z. Wen, C. Li, D. Wu, A. Li, N. Ming, *Nature Mater.* **2013**, 12, 617.

18. X. Li, Y. Zhu, W. Cai, M. Borysiak, B. Han, D. Chen, R. D. Piner, L. Colombo, R. S. Ruoff, *Nano Lett.* **2009**, 9, 4359.

19. A. A. Balandin, S. Ghosh, W. Bao, I. Calizo, D. Teweldebrhan, F. Miao, C. N. Lau, *Nano Lett.* **2008**, 8, 902.

20. Y. Zhao, Y. Xie, Y. Y. Hui, L. Tang, W. Jie, Y. Jiang, L. Xu, S. P. Lau, Y. Chai, *J. Mater. Chem. C* **2013**, 1, 4956.

21. W. Jie, J. Hao, *Nanoscale* **2014**, 6, 6346.

22. S. Yuan, Z. Yang, C. Xie, F. Yan, J. Dai, S. P. Lau, H. L. W. Chan, J, Hao, *Adv. Mater.* **2016**, 28, 10048.

26. M. Oku, K. Wagatsuma, S. Kohiki, *Phys. Chem. Chem. Phys.* **1999**, 1, 5327.

27. V. Garcia, M. Bibes, L. Bocher, S. Valencia, F. Kronast, A. Crassous, X. Moya, S.

23. J. Hao, W. Si, X. X. Xi, R. Guo, A. S. Bhalla, L. E. Cross, *Appl. Phys. Lett.* **2000**, 76, 3100.

24. J. H. Hao, J. Gao, Z. Wang, D. P. Yu, *Appl. Phys. Lett.* **2005**, 87, 131908.

25. X. Wang, B. Song, L. L. Tao, J. Wen, L. Zhang, Y. Zhang, Z. Lv, J. Tang, Y. Sui, B. Song, X. F. Han, *Appl. Phys. Lett.* **2016**, 109, 163501.

26. M. Oku, K. Wagatsuma, S. Kohiki, *Phys. Chem. Chem. Phys.* **1999**, 1, 5327.

27. V. Garcia, M. Bibes, L. Bocher, S. Valencia, F. Kronast, A. Crassous, X. Moya, S.

Enouz-Vedrenne, A. Gloter, D. Imhoff, C. Deranlot, N. D. Mathur, S. Fusil, K. Bouzehouane, A. Barthélémy, *Science* **2010**, 327, 1106.

28. G. Radaelli, D. Gutiérrez, F. Sánchez, R. Bertacco, M. Stengel, J. Fontcuberta, *Adv. Mater*. **2015**, 27, 2602.

29. Z. Xi, J. Ruan, C. Li, C. Zheng, Z. Wen, J. Dai, A. Li, D. Wu, *Nature Commun*. **2017**, 8, 15217.

38
39
40
41
42
43
44
45

Figures and captions

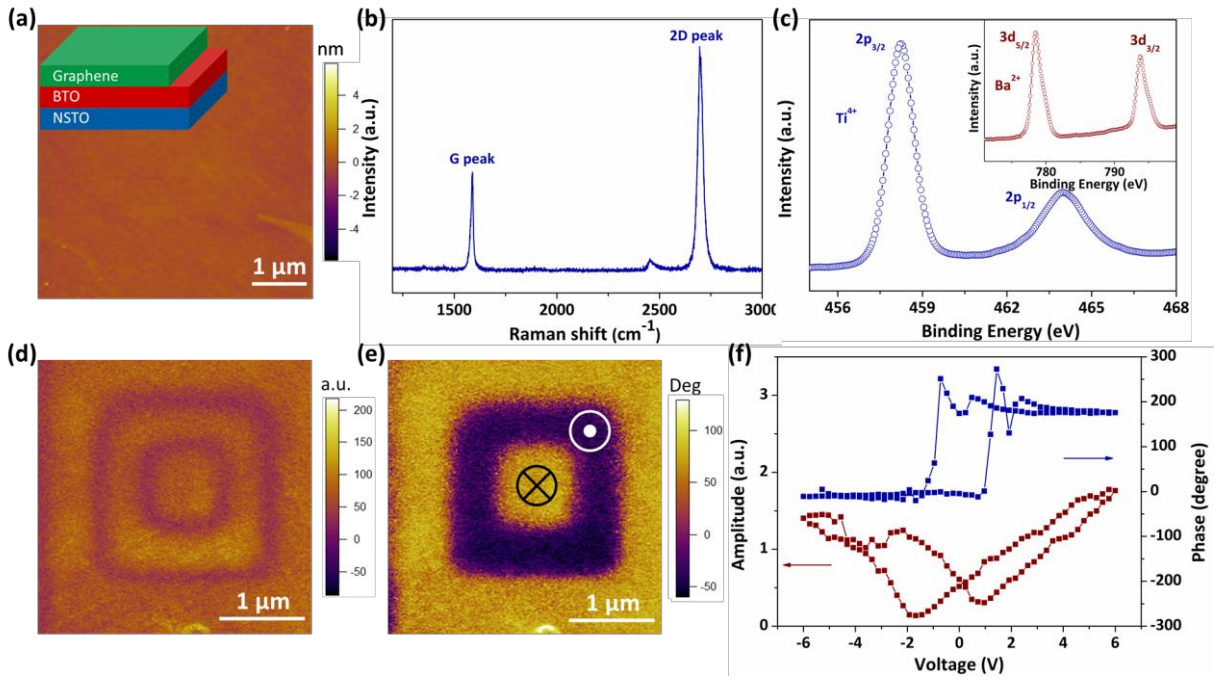

Figure 1. (a) Topography of graphene/BTO/NSTO heterostructure. Inset is the schematic device geometry. (b) Raman spectrum of the CVD-grown monolayer graphene. (c) XPS measurement of the BTO thin film. PFM out-of-plane amplitude (d) and phase (e) images of square domains with opposite polarization orientation written on the BTO/NSTO surface after applying a positive and negative DC voltage of 3 V. (f) Local PFM hysteresis loops: phase

signal (top) and amplitude signal (bottom).

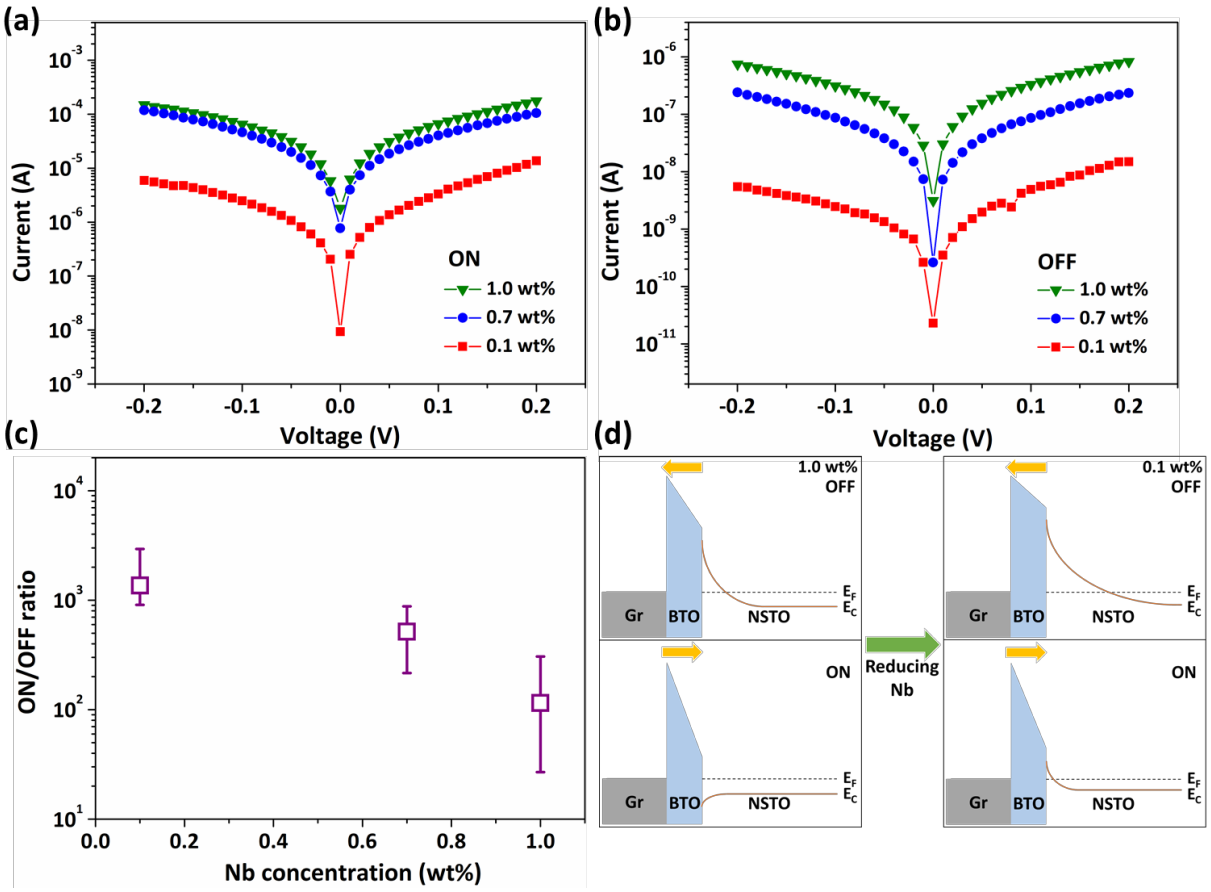

Figure 2. The room-temperature *I-V* curves of the graphene/BTO/NSTO heterostructure with various Nb doping concentration of semiconductor substrates in (a) the ON and (b) the OFF states. (c) ON/OFF ratio of the devices as a function of Nb concentration. The error bars

present the average measured in 10 different device points for each Nb concentration. (d) Schematic illustration of the energy barrier diagram for the ON and OFF states with different Nb doping concentration. The Gr symbol represents graphene layer. The yellow arrows denote the polarization directions in the BTO barrier.

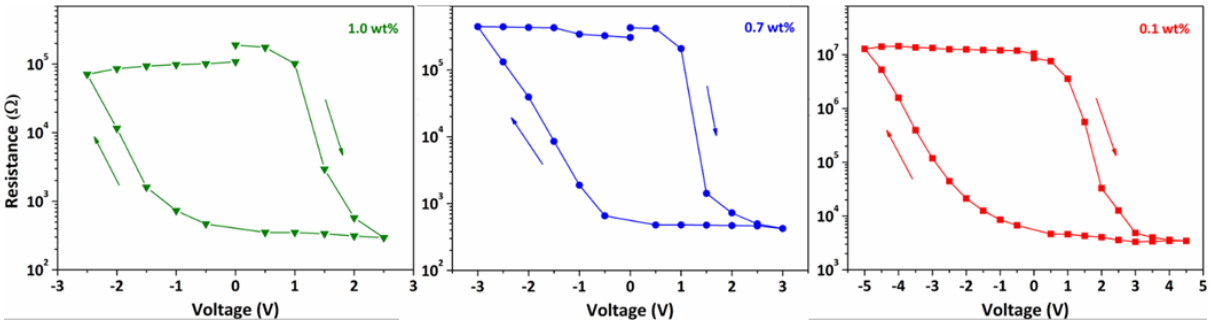

Figure 3. The room-temperature *R-V* hysteresis loops of graphene/BTO/NSTO heterostructure as a function of Nb doping concentration in NSTO substrates: 1.0 wt% (left), 0.7 wt% (middle), and 0.1 wt% (right).

37
38
39
40
41
42
43
44
45

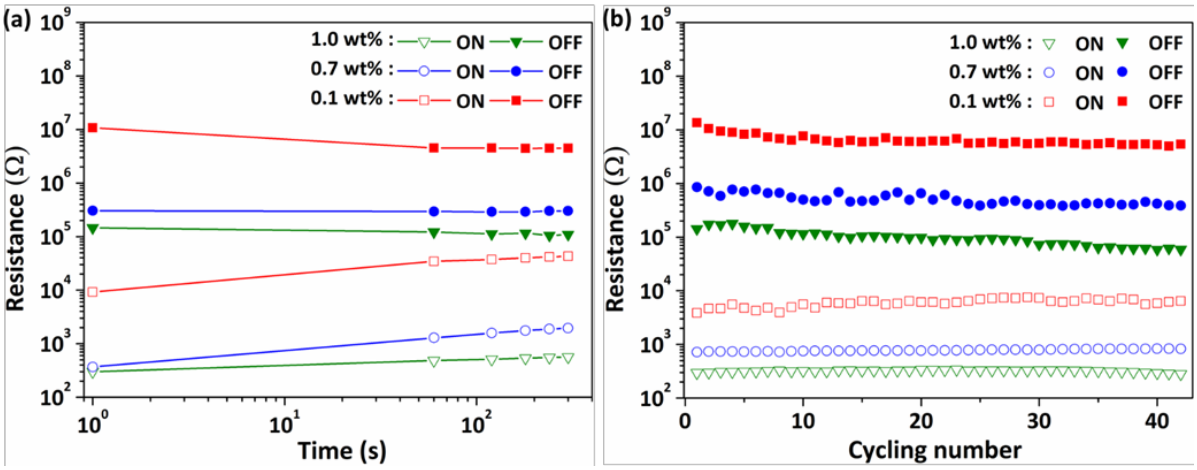

Figure 4. (a) Data retention and (b) bipolar resistance switching of graphene/BTO/NSTO heterostructure with different Nb doping concentration in semiconducting NSTO substrates at room temperature.

Table of contents entry

A novel FTJ employing both two-dimensional material and semiconductor electrode has been developed. It is found that the ON/OFF resistance ratio of graphene/$BaTiO_3$/Nb:$SrTiO_3$ heterostructure increases with decreasing Nb concentration in the semiconductor electrode. An optimized ON/OFF ratio above 10^3 is obtained at 0.1 wt% Nb concentration. Moreover, good retention property and switching reproducibility are observed in the ferroelectric tunneling devices, which may faciliate the design of memory application.

Keywords: two-dimensional materials, pulsed laser deposition, ferroelectric tunnel junctions, tunneling electroresistance effect, graphene-based devices

Hung-Lit Chan, Shuoguo Yuan, and Jianhua Hao*

Vertical Graphene Tunneling Heterostructure with Ultrathin Ferroelectric $BaTiO_3$ Film as a Tunnel Barrier